Journal of CO2 Utilization **2020, *Volume 57*, 101884,**
DOI: https://doi.org/10.1016/j.jcou.2022.101884
https://www.sciencedirect.com/science/article/pii/S2212982022000038

Carbon Nanotube Supported Aluminum Porphyrin-Imidazolium Bromide Crosslinked Copolymer: A Synergistic Bifunctional Catalyst for CO_2 Conversion

Vincenzo Campisciano,[a] Laura Valentino,[a] Anthony Morena,[a,b] Andrea Santiago Portillo,[b] Nicolò Saladino,[a] Michelangelo Gruttadauria,*[a] Carmela Aprile,*[b] and Francesco Giacalone*[a]

[a] Department of Biological, Chemical and Pharmaceutical Sciences and Technologies, University of Palermo, Viale delle Scienze, Ed. 17 90128, Palermo (Italy) E-mail: francesco.giacalone@unipa.it, michelangelo.gruttadauria@unipa.it

[b] Laboratory of Applied Material Chemistry (CMA), Department of Chemistry, University of Namur, 61 rue de Bruxelles 5000, Namur (Belgium) E-mail: carmela.aprile@unamur.be

Keywords: Carbon dioxide fixation • bifunctional catalyst • Al-porphyrin • cyclic carbonates • carbon nanotubes

Abstract: The increased awareness of the catastrophic consequences caused by the accumulation of greenhouse gases into the atmosphere has generated a large mobilization aimed at CO_2 mitigation. Herein, in the spirit of the transformation of a waste as CO_2 into value added products, we propose an efficient preparation of two different hybrid systems based on aluminum chloride tetrastyrylporphyrin (TSP-Al-Cl) and 1,4-butanediyl-3,3′-bis-1-vinylimidazolium dibromide copolymerized in the presence (MWCNT-TSP-AlCl-imi) and in absence (TSP-AlCl-imi) of multi-walled carbon nanotubes (MWCNTs) for the CO_2 utilization in the synthesis of cyclic carbonates. The so-prepared materials have been thoroughly characterized by means of several spectroscopic and analytical techniques. The MWCNT-TSP-AlCl-imi heterogenous catalyst enabled the highly efficient chemical transformation of CO_2 and epoxides into cyclic carbonates with high turnover number (TON) and frequency (TOF) values at low temperature down to 30 °C in solvent-free conditions. MWCNT-TSP-AlCl-imi proved to be a very stable and reusable heterogeneous catalyst in consecutive cycles without the need of any reactivation procedure and no leaching phenomena. Furthermore, the optimal morphology of MWCNT-TSP-AlCl-imi, with the crosslinked polymer uniformly distributed onto MWCNTs backbone, resulted in a more active catalyst with a TON double than the unsupported one. The enhanced activity of MWCNT-TSP-AlCl-imi can be ascribed to its higher surface area that permits fully accessible catalytic sites. Interestingly, MWCNT-TSP-AlCl-imi also showed a catalytic activity comparable to a reference homogeneous catalytic system, proving that synergism occurred between the metal centers and the nucleophilic sites due to their close proximity.

Introduction

The intensive use of fossil fuels is the main cause of the large emissions of carbon dioxide into the atmosphere. Nevertheless, if on the one hand CO_2, with its huge contribution to the greenhouse effect, is

responsible for the drastic climate change we are witnessing nowadays, on the other hand it is also a low-priced, abundant, and sustainable C_1 resource for the chemical industry.[1-4] It is therefore not surprising that the transformation of a waste as CO_2 into useful products represents a topic of current interest that meets the requirements both from the environmental and industrial viewpoint. Among the wide range of CO_2-derived high-value added chemicals, the cycloaddition of carbon dioxide with epoxides for the synthesis of cyclic carbonates, which find applications as chemical intermediates, polar aprotic solvents, or battery electrolytes, have aroused a great research interest.[5-7] However, due to the highly stable and inert nature of CO_2, the synthesis of cyclic carbonates starting from epoxides has required the development of efficient catalytic systems, both homogeneous and heterogeneous, able to promote the chemical conversion of carbon dioxide under ever milder reaction conditions.[8-12] Undoubtedly, although homogeneous catalysts offer remarkable advantages, such as high activity and selectivity, they suffer from certain drawbacks mainly related to their difficult recycling/reuse and laborious purification processes of cyclic carbonates from the reaction medium, which may represent highly time- and energy-consuming procedures. The solution to those issues lies in the preparation of heterogeneous catalytic systems that can certainly make the recycling process and their reuse much easier. Heterogeneous metal-based catalysts are a class of materials extensively exploited in the chemical transformation of CO_2 into cyclic carbonates. The presence of the metal center is responsible for the activation of the epoxide enabling the conversion of CO_2 under milder reaction conditions. By taking the last approach, the appeal of the overall catalytic process is considerably increased becoming highly sustainable. It deserves to be mentioned that the conversion of CO_2 into cyclic carbonates fulfils various principles of green chemistry such as the transformation of a waste and a renewable source in high values-added chemicals, 100% atom economy, the possibility to perform the process under solvent-free conditions and with the help of a heterogeneous catalyst. This has prompted the scientific community to develop different metal-based catalysts active in the synthesis of cyclic carbonates and including metal oxides,[13-17] metal-organic frameworks (MOFs),[18-23] zeolites,[24-30] as well as porous organic polymers (POPs)[11, 19, 31] and covalent organic frameworks (COFs)[32] with accessible metal sites, among others. Most of the metal-based catalytic systems require the presence of additional nucleophilic co-catalytic species, such as tetrabutylammonium bromide (TBAB), which can help in the ring-opening of the epoxides, though used, in some cases, in very large amount with respect to metal catalyst, leading to incorrect TOF values.[33] In such a way, both the electrophilic/Lewis acid and the nucleophilic/Lewis base centers can simultaneously cooperate contributing to improve the catalytic efficiency. However, if on the one hand the use of a nucleophilic additive can enhances the performance towards the conversion of CO_2, on the other hand the presence of an external component could cause a detrimental effect in terms of complexity of the reaction mixture and difficulty of the purification process of cyclic carbonates.[22] Therefore, a possible solution to this issue could be offered by the preparation of a heterogeneous bifunctional catalyst containing both the metal center and the nucleophilic species. In this context, a rational design of the heterogeneous catalyst at the molecular scale is of paramount importance. For this purpose, metalloporphyrin complexes represent ideal molecular scaffolds since the porphyrin core can be properly functionalized in order to

improve the activity of the final catalyst. The high versatility of these complexes, together with that of another highly exploited class of complex, namely Salen-based metal complexes, is witnessed by their widespread use in the cycloaddition of CO_2 with epoxides. Various complexes based on many metals, such as Zn, Al, Mg, Ni, Cr, and Co have been incorporated in the structure of different heterogeneous catalysts used for this aim. In particular, these metal-based catalysts can be classified into two types, namely those requiring the addition of an external nucleophilic co-catalytic species[34-46] and those belonging to the bifunctional type.[47-69] Therefore, in the light of above and on the basis of our experience with imidazolium salts-based catalysts for the conversion of CO_2 into cyclic carbonates,[70-77] we designed the preparation of a bifunctional and efficient heterogeneous catalyst for CO_2 fixation into epoxides. The approach for the obtaining of the target catalytic material consisted in the preparation of a porous structure synthesized from the radical copolymerization of a tetrastyrylporphyrin aluminum chloride (**TSP-AlCl**) monomer with a bis-vinylimidazolium (**bis-imi**) salt bearing bromide anion as counter ion. In such a way, a fixed local concentration of active sites corresponding to an Al/Br^- ratio of 1/8 and a fine control over their relative position to maximize the cooperation/synergism between the electrophilic and nucleophilic sites has been reached. Another crucial factor is to ensure easy access of the reagents to active sites. The highly cross-linked nature of the hybrid prepared generates a material with a low surface area, and this could drastically reduce the diffusion rate of the reactants towards the active sites eventually causing a lowering of the catalytic activity. Therefore, a support material onto which the polymeric network can be uniformly distributed and can at the same time make all the catalytic sites fully accessible and impart robustness to the entire catalytic system is highly desired. In our previous works, we have shown how different carbon nanoforms (CNFs) can direct the growth of polymers, which eventually formed a uniform coating around the carbonaceous skeletons.[72, 73, 78-80] In addition, the functionalization of CNFs by means of radical polymerization represents a very efficient strategy in terms of both the intrinsically inherent near 100% atom economy of reaction mechanism of the polymerization process, and the limited production of waste due to the excellent yields and high functionalization degree of the so-obtained CNFs (low E-factor). Therefore, herein we have chosen multi-walled carbon nanotubes (MWCNTs) as ideal support material onto which to build the polymeric network of **TSP-AlCl** and **bis-imi**. All the materials prepared and their precursors have been fully characterized by means of different techniques, and the heterogeneous bifunctional Al/Br^- catalyst supported onto MWCNTs has been tested in the synthesis of cyclic carbonates starting from CO_2 and several epoxides with excellent results.

Materials and methods

Styrene oxide, epichlorohydrin and cyclohexene oxide were purchased from TCI. Glycidol, limonene oxide, 1,4-butanediol diglycidyl ether and 2,2′-Azobis(2-methylpropionitrile) (AIBN) were purchased from Sigma-Aldrich. These chemicals were used without further purification. Transmission electron microscopy (TEM) images were obtained using a Philips Tecnai 10 microscope operating at 80 kV. The samples were prepared by dispersion of a small quantity of the material in absolute ethanol and deposited into a copper grid. X-ray

photoelectron spectroscopy (XPS) analysis were carried out in a ThermoFisher ESCALAB 250Xi instrument. Inductively coupled plasma optical emission spectroscopy (ICP-OES) were performed in an Optima 8000 ICP-OES Spectrometer. Nitrogen adsorption analysis were carried out in a Micromeritics Tristar 3000 and ASAP 2000. The material was pre-treated at 150 ºC for 16 h under reduced pressure. The Brunauer-Emmett-Teller (BET) method as applied in the 0.05-0.30 p/p_0 range to calculate the specific surface area. Thermogravimetric analysis was performed under nitrogen flow from 25 to 900 ºC with a heating rate of 10 ºC/min in a Mettler Toledo TGA STAR system. Chemical combustion analysis was performed on a Perkin-Elmer 2400 Serie 2 analyzer. ^{1}H and ^{13}C NMR spectra were recorded on a Bruker 300 MHz spectrometer. Solid state ^{13}C and ^{29}Si NMR spectra were recorded at room temperature on a Bruker Avance-500 spectrometer operating at 11.7 T using a 4.0 mm probe and spinning frequencies of 8 and 10 kHz.

Synthetic procedures

Synthesis of bisvinylimidazolium salt (bis-imi). In a 10 mL round bottom flask, a solution of 1,4-dibromobutane (950 µL, 7.88 mmol) and 1-vinylimidazole (1.5 mL, 16.24 mmol) in methanol (2 mL) was stirred in the dark and under Ar atmosphere at 65 °C for 13 h. The solution was transferred in a 100 mL round bottom flask and the volume was reduced under vacuum before adding Et_2O (70 mL). After sonication and vigorous stirring, a white precipitate was obtained and the supernatant was removed by simple decantation. Afterwards, methanol (2 mL) was added and gently warmed to solubilize the solid obtaining a yellowish viscous oil, which again after the addition of diethyl ether and sonication gave rise to a white precipitate. Diethyl ether was then removed and the whole procedure of solubilization in methanol and precipitation with diethyl ether was repeated twice. The obtained white solid was dried under vacuum at 40 °C. bis-imi was obtained as a white solid (3.128 g; 98%).

Synthesis of 4-vinylbenzaldehyde (2). 4-Vinylbenzaldehyde was synthesized according to a reported procedure.[81] In a 100 mL two-neck round-bottom flask, under Ar atmosphere, Mg (550 mg, 22.63 mmol), a catalytic amount of I_2 and dry THF (28 mL) were transferred. The mixture was allowed to stir at 30 °C for 30 minutes before the dropwise addition of 4-bromostyrene 1 (2 mL, 14.53 mmol). The temperature was gradually increased up to 67 °C and the reaction mixture was reacted at this temperature for 2 h. Dry DMF (3.4 mL) was added at 0°C and stirred at room temperature overnight. The reaction mixture was quenched with a saturated NH_4Cl solution (15 mL), filtered to remove any insoluble residue, and extracted with ethyl acetate. The combined organic phases were dried over $MgSO_4$, filtered, concentrated under vacuum (at room temperature to avoid the polymerization of 4-vinylbenzaldehyde), and purified by column chromatography on silica gel (hexane/ethyl acetate (v/v): 30/1). The 4-vinylbenzaldehyde was obtained as yellowish oil (1.496 g; 78%). ^{1}H NMR (300 MHz, CDCl3, δ): 7.86 (d, J = 8.2 Hz, 2H), 7.57 (d, J = 8.2 Hz, 2H), 6.79 (dd, J = 17.6, 10.9 Hz, 1H), 5.93 (d, J = 17.6 Hz, 1H), 5.46 (d, J = 10.9 Hz, 1H) ppm.

Synthesis of tetrastyrylporphyrin (TSP). Tetrastyrylporphyrin (**TSP**) was synthesized according to a reported procedure.[39] In a 250 mL two-neck round-bottom flask propionic acid (104 mL) was heated to 140 °C in air before adding fresh distilled pyrrole (795 µL, 11.34 mmol) and 4-vinylbenzaldehyde (1.496 g, 11.32 mmol). After 5 h the reaction mixture was allowed to reach room temperature and then the two-neck round-bottom flask was placed in an ice bath before filtering and washing with methanol and ethyl acetate. After drying, the tetrastyrylporphyrin was obtained as purple crystals (600 mg, 29%). ^{1}H NMR (300 MHz, $CDCl_3$, δ): 8.90 (s, 8H), 8.19 (d, *J* = 7.9 Hz, 8H), 7.81 (d, *J* = 8.0 Hz, 8H), 7.07 (dd, *J* = 17.6, 10.9 Hz, 4H), 6.08 (d, *J* = 17.6 Hz, 4H), 5.51 (d, *J* = 10.9 Hz, 4H), -2.73 (s, 2H) ppm. ^{13}C NMR (75 MHz, $CDCl_3$, δ): 141.69, 136.94, 136.71, 134.83, 124.61, 119.90, 114.67 ppm. FT-IR (film): 3328, 2920, 2853, 1827, 1627, 1602, 1557, 1504, 1471, 1401, 1349, 1219, 1185, 1154, 1112, 1017, 987, 966, 911, 854, 803, 727 cm^{-1}. UV−vis: ($CHCl_3$) λmax (ε) = 420 (379950), 517 (14900), 553 (9375), 591 (4825), 647 (4700) nm.

Synthesis of tetrastyrylporphyrin aluminum chloride (TSP-AlCl). In a 50 mL two-neck round-bottom flask, under Ar atmosphere, tetrastyrylporphyrin (570 mg, 0.79 mmol), and dry DCM (11.4 mL) were charged. The mixture was cooled to 0 °C by means of an ice bath and then a solution of diethylaluminum chloride (25 wt% solution in toluene, 490 µL, 0.90 mmol) was slowly added. Then the reaction mixture was allowed to reach the room temperature and stirred for 6 h before transferring it in a centrifuge tube and adding methanol. Four centrifugations with methanol were carried out and the combined supernatants were evaporated under vacuum. The residue was taken up with DCM and all the insoluble residues were removed by filtration. The filtrate was concentrated under vacuum and TSP-AlCl was obtained as purple powder (293 mg, 47%). ^{1}H NMR (300 MHz, $CDCl_3$, δ): 8.41 (s, 8H), 7.49 (s, 16H), 6.98 (dd, *J* = 17.6, 11.0 Hz, 4H), 5.99 (d, *J* = 17.7 Hz, 4H), 5.49 (d, *J* = 10.9 Hz, 4H) ppm. ^{13}C NMR (75 MHz, $CDCl_3$, δ): 146.72, 140.77, 136.70, 136.62, 134.32, 131.12, 124.38, 119.33, 114.62 ppm. FT-IR (film): 2922, 2853, 1627, 1496, 1402, 1351, 1293, 1236, 1209, 1012, 911, 801, 726 cm^{-1}. UV−vis: ($CHCl_3$) λmax (ε) = 422 (138250), 517 (2075), 552 (4675), 595 (1900), 646 (525) nm.

Preparation of MWCNT-TSP-AlCl-imi. In a 25 mL two-neck round-bottom flask, MWCNTs (97 mg), **TSP-AlCl** (146 mg, 0.19 mmol), bis-vinylimidazolium salt **bis-imi** (303 mg, 0.75 mmol), and absolute ethanol (9.7 mL) were transferred and sonicated for 20 minutes. Then, under Ar atmosphere, AIBN (51 mg, 0.31 mmol) was added and Ar was bubbled in the reaction mixture while stirring for 30 minutes at room temperature. The temperature was gradually increased up to 78 °C and the reaction mixture was allowed to react at this temperature for 15 h. The dark viscous residue obtained was transferred in a centrifuge tube adding a mixture of methanol/Et_2O (v/v) 2/1. The residue was subjected to centrifugation, three times using the methanol/Et_2O (v/v) 2/1 mixture, one time with a methanol/Et_2O (v/v) 1/1 mixture, and three additional times with pure Et_2O. The residue was recovered and dried under vacuum at 40 °C. **TSP-AlCl-imi-MWCNT** was obtained as a dark powder (463 mg). FT-IR (KBr pellet): 3417, 3123,3085, 2920, 2850, 1627, 1552, 1454, 1157, 1011, 807, 738, 653 cm^{-1}. CHN analysis (%): C 59.7; H 4.9; N 8.6.

Preparation of TSP-AlCl-imi. In a 25 mL two-neck round-bottom flask, under Ar atmosphere, TSP-AlCl (250 mg, 0.32 mmol), bis-vinylimidazolium salt **bis-imi** (518 mg, 1.28 mmol), AIBN (21 mg, 0.13 mmol), and absolute ethanol (5.0 mL) were transferred. Then, Ar was bubbled in the reaction mixture while stirring for 20 minutes at room temperature. The temperature was gradually increased up to 78 °C and the reaction mixture was allowed to react at this temperature for 15 h. The solvent was removed und er vacuum and the residue was washed by soxhlet extraction with methanol overnight. After oven-drying at 60 °C, **TSP-AlCl-imi** was obtained as dark powder (576 mg). FT-IR (KBr pellet): 3403, 3132, 3085, 2933, 2868, 1627, 1553, 1501, 1451, 1351, 1208, 1157, 1011, 859, 805, 748 cm^{-1}. CHN analysis (%): C 50.5; H 5.6; N 10.5.

Synthesis of tetraphenylporphyrin (TPP). Tetraphenylporphyrin (**TPP**) was synthesized according to a reported procedure.[44] In a 250 mL two-neck round-bottom flask propionic acid (90 mL) was heated to 140 °C in air before adding fresh distilled pyrrole (650 µL, 9.27 mmol) and 4-vinylbenzaldehyde (950 µL, 9.25 mmol). After 5 h the reaction mixture was allowed to reach room temperature and then the two-neck round-bottom flask was placed in an ice bath before filtering and washing with methanol and ethyl acetate. After drying, the tetraphenylporphyrin was obtained as purple crystals (299 mg, 21%). Spectroscopic data are in accordance with those reported in literature.[44]

Synthesis of tetraphenylporphyrin aluminum chloride (TPP-AlCl) complex. Tetraphenylporphyrin aluminum chloride (**TPP-AlCl**) complex was synthesized according to a reported procedure.[44] in a 50 mL two-neck round-bottom flask, under Ar atmosphere, tetraphenylporphyrin (90 mg, 0.15 mmol), and dry DCM (2.1 mL) were charged. The mixture was cooled to 0 °C by means of an ice bath and then a solution of diethylaluminum chloride (25 wt% solution in toluene, 90 µL, 0.16 mmol) was slowly added. Then the reaction mixture was allowed to reach the room temperature and stirred for 6 h before transferring it in a centrifuge tube and adding methanol. Four centrifugations with methanol were carried out and the combined supernatants were evaporated under vacuum. The residue was further purified by a short column chromatography on silica gel (DCM/methanol (v/v): 10/1). The **TPP-AlCl** was obtained as purple powder (48 mg, 47%). Spectroscopic data are in accordance with those reported in literature.[44]

Catalytic experiments

Catalytic experiments were performed in a Cambridge Design Bullfrog batch reactor with temperature control and mechanical stirring. In this reactor, also pressure can be monitored. Before each experiment, the material was dried overnight in a vacuum oven at 60 ºC. In each test, the catalyst was added to 24 mL of epoxide in a Teflon vial under solvent free conditions. After closing the reactor, the mixture was stirred at 500 rpm. The system was then purged for 10 min with N_2 before the addition of 25 bar of CO_2. After this, the system was heated to the required temperature with a rate of 5 ºC/min. The reaction mixture was kept to the required temperature during the reaction time. When needed a refill of CO_2 was performed during the experiment to preserve the amount of reactant required for the reaction. In any case the pressure of CO_2 added overpasses the initial pressure reached at the temperature of the experiment. After this time, the

reactor was cooled down to room temperature and then it was depressurized. The catalyst was separated from the reaction mixture via centrifugation during 30 min at 4500 rpm and the supernatant was analyzed by ^{1}H NMR in $(CD_3)_2SO$.

Recycling test

Recycling test were carried out in the reaction of styrene oxide with CO_2. At the end of the reaction, the material was recovered by centrifugation and washed several times with 45 mL of toluene, ethanol and one time with diethyl ether. Moreover, each time the catalyst was previously sonicated with the washing solvent. Then, before the next cycle, the catalyst was dried overnight in a vacuum oven at 60 ºC. After drying, the catalyst was reused in the same reaction maintaining the ratio between moles of catalyst and moles of epoxides.

Leaching test

Leaching test was performed in the reaction of styrene oxide with CO_2. Once the reaction time passed, the reactor was cooled down to room temperature and then it was depressurized. As usually, the catalyst was separated from the reaction mixture via centrifugation during 30 min at 4500 rpm and the supernatant was analyzed by ^{1}H NMR in $(CD_3)_2SO$. Then, the remaining supernatant (without catalyst) was introduced again into the reactor. As in a normal reaction, the system was then purged for 10 min with N_2 before the addition of 25 bar of CO_2 and the increase of the temperature with a rate of 5 ºC/min. The reaction mixture was kept to the selected temperature for the required time. During the reaction time, no decrease of the CO_2 pressure was observed and no further conversion was detected by ^{1}H NMR analysis.

Results and discussion

The formylation of the Grignard reagent arising from 4-bromostyrene **1** gave rise to 4-vinylbenzaldehyde **2** that was reacted with pyrrole in propionic acid to obtain tetrastyrylporphyrin (**TSP**). The following reaction of **TSP** with Et_2AlCl led to the formation of tetrastyrylporphyrin aluminum chloride (**TSP-AlCl**) complex. **TSP-AlCl** was afterwards copolymerized with the bis-vinylimidazolium salt **bis-imi** to produce the copolymer **TSP-**

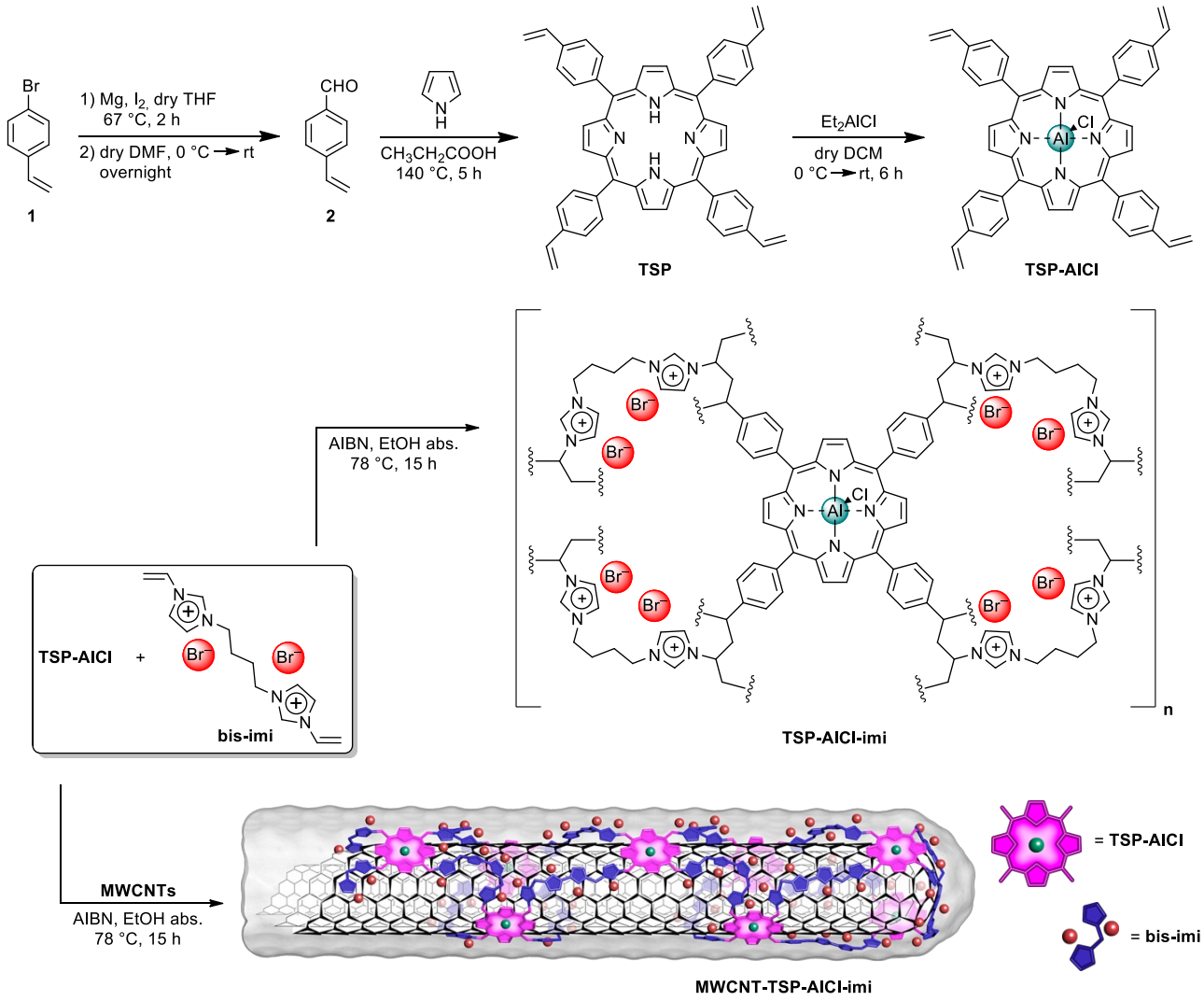

Scheme 1 Synthetic procedure for the preparation of **TSP-AlCl-imi** and **MWCNT-TSP-AlCl-imi**.

AlCl-imi, or **MWCNT-TSP-AlCl-imi** when MWCNTs were used as support material (**Scheme 1**).**TSP** and **TSP-AlCl** were firstly analyzed by means of FT-IR spectroscopy (**Figure 1**). The spectrum of **TSP** (**Figure 1**, black line) shows the typical bands associated with the free base porphyrin derivatives[82-84] including the weak band centered at 3328 cm^{-1} ascribed to the N–H stretching, two bands at 1602 and 1557 cm^{-1} due to the pyrrole rings stretching vibrations, a band of medium intensity at 1471 cm^{-1} generated by the C–N–C bending, two bands at 987 and 966 cm^{-1} due to the asymmetric breathing motions of the pyrrole rings, and a strong absorption band at 803 cm^{-1} attributed to the N–H *out-of-plane* bending vibration mode. The disappearance of these absorptions in the **TSP-AlCl** spectrum and the presence of a new strong absorption centered at 1012 cm^{-1} due to the porphyrin ring vibration in the metal complex (**Figure 1**, red line) confirmed the aluminum insertion into the porphyrin ring.

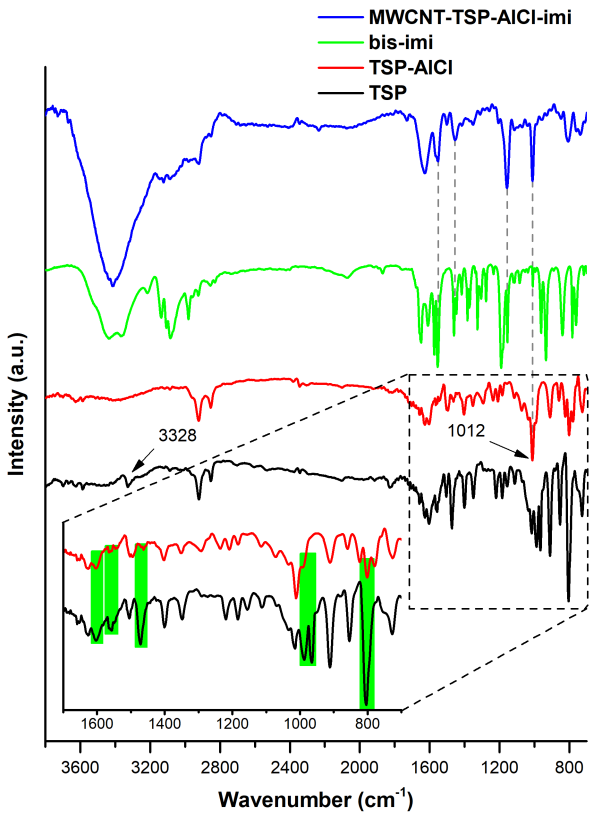

Fig. 1 FT-IR spectra of **TSP** (black line), **TSP-AlCl** (red line), **bis-imi** (green line), and **MWCNT-TSP-AlCl-imi** (KBr pellet; blue line).

UV-Vis spectrum of the free-base **TSP** (**Figure 2**, dashed black line) exhibits a series of bands in the 370-450 nm and 480-680 nm regions due to π-π* transitions. The absorption at 420 nm is associated with the Soret band ($S_0 \rightarrow S_2$), whereas the Q-bands ($S_0 \rightarrow S_1$) are shown in the magnification of **Figure 2** at 517, 553, 591, and 647 nm.[85] The complexation of the metal center resulted in a slightly red-shifted Soret band of **TSP-AlCl** at 422 nm (**Figure 2**, red line). However, as previously reported for similar Al(III)porphyrin derivatives,[41] the UV-Vis spectrum of **TSP-AlCl** was still characterized by the presence of four Q-bands but with different relative intensities (**Figure 2**).

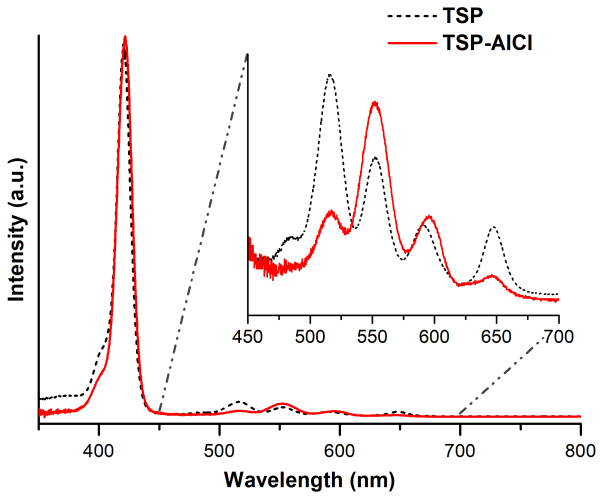

Fig. 2 UV-Vis spectra of **TSP** (dashed black line), and **TSP-AlCl** (red line) in $CHCl_3$.

In addition, further evidence of the successful insertion of Al center into tetrastyrylporphyrin was provided by NMR spectroscopy (**Figures S1-S4**). In particular, the comparison of **TSP** and **TSP-AlCl** ^{1}H NMR spectra shows the disappearance of the pyrrolic protons resonating at -2.73 ppm after the complexation step (**Figure S1** and **S3**).

As stated before, the copolymerization of **TSP-AlCl** with **bis-imi** gave **TSP-AlCl-imi**, whereas **MWCNT-TSP-AlCl-imi** was obtained when the copolymerization was carried out in the presence of MWCNTs as support. Both materials **TSP-AlCl-imi** and **MWCNT-TSP-AlCl-imi** were fully characterized by means of different techniques.

Once again, FT-IR spectroscopy has proved to be a useful tool for providing the first evidence of the successful copolymerization process, and the comparison of **MWCNT-TSP-AlCl-imi** spectrum (**Figure 1**, blue line), with those of **TSP-AlCl-imi** (red line) and **bis-imi** (green line) confirmed the presence of the Al porphyrin complex and bis-vinylimidazolium salt in the material **MWCNT-TSP-AlCl-imi**. The strong absorption at 1012 cm^{-1}, which is typical of **TSP-AlCl**, and the medium intensity absorptions at 1551, 1454, and 1157 cm^{-1}, associated with the imidazolium ring stretching vibration modes,[78, 86] can be detected in the FT-IR spectrum of **MWCNT-TSP-AlCl-imi** (**Figure 1**, compare blue line with red and green lines). The high hygroscopicity of the copolymerized imidazolium-based salt causes the presence of the very strong and broad absorption band at 3415 cm^{-1} due to the O–H stretch, and the medium absorption at 1628 cm^{-1} generated by the H–O–H bending of the adsorbed water. The FT-IR spectrum of **TSP-AlCl-imi** (**Figure S5**) showed no remarkable difference from that of **MWCNT-TSP-AlCl-imi**.

Materials **MWCNT-TSP-AlCl-imi** and **TSP-AlCl-imi** were further characterized by means of ^{13}C cross-polarization magic angle spinning (^{13}C CPMAS) NMR spectroscopy (**Figure 3**). Both spectra show the signals attributed to the resonance of the carbon atoms of the porphyrin core along with those of the imidazolium moieties in the 115-150 ppm region, whereas the signals ascribed to the aliphatic carbon atoms resonate in the upfield part of the spectra (20-60 ppm). Further proof of the good outcome of the

polymerization was provided by the absence of any signal in the 100-115 ppm region where carbon atoms of vinyl group resonate.

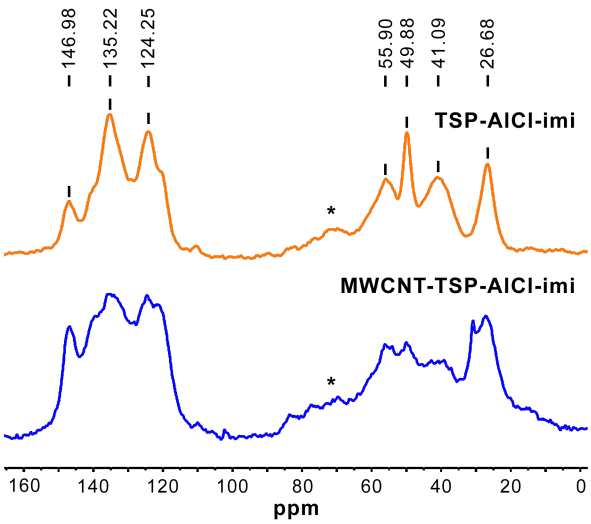

Fig. 3 ^{13}C CP-MAS NMR of **TSP-AlCl-imi** (orange line) and **MWCNT-TSP-AlCl-imi** (blue line). Asterisks indicate spinning side bands.

X-ray photoelectron spectroscopy (XPS) analysis was used to analyze the outer surface of materials **MWCNT-TSP-AlCl-imi** and **TSP-AlCl-imi** (**Figure 4** and **S6**). The survey spectrum of **MWCNT-TSP-AlCl-imi** (**Figure 4a**) confirm the presence of Al and Br arising from the **TSP-AlCl** and **bis-imi** monomers, respectively. The high-resolution XPS spectra of the N1s region of **MWCNT-TSP-AlCl-imi** (**Figure 4b**) can be deconvoluted into two peaks at 399.1 and 401.3 eV with atomic percentages of 34.4% and 65.6% corresponding to the nitrogen atoms of the porphyrin ring coordinated with aluminum (Al–N)[44] and the nitrogen atoms of the imidazolium rings,[87] respectively. The atomic percentages of the two different nitrogen atoms in **TSP-AlCl-imi** correspond to 18.0% and 82.0% for Al–N and imidazolium-N, respectively (**Figure S6**).

Thermogravimetric analysis of **MWCNT-TSP-AlCl-imi** and **TSP-AlCl-imi** under nitrogen atmosphere was used to assess the good thermal stability of the materials. With the exception of the initial weight loss between room temperature and 100 °C due to the adsorbed moisture, the materials proved to be very stable up to 250 °C (**Figure 5**), at which temperature they start to degrade with a first weight loss centered at about 320 °C for both materials, and a second degradation peak centered at 438 and 462 °C for **MWCNT-TSP-AlCl-imi** and **TSP-AlCl-imi**, respectively. Conversely, TGA under nitrogen of pristine MWCNT showed only a 3% weight loss at 700 °C (**Figure 5**, black line).

The Al content of **MWCNT-TSP-AlCl-imi** (0.251 mmol/g) and **TSP-AlCl-imi** (0.444 mmol/g) was determined by means of inductively coupled plasma atomic emission spectroscopy (ICP-OES) analysis.

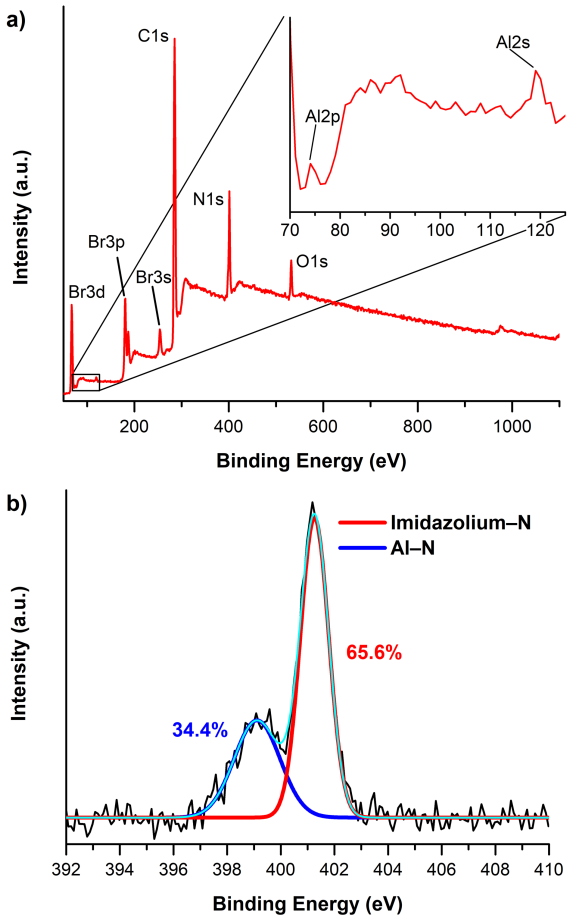

Fig. 4 a) XPS survey spectrum of **MWCNT-TSP-AlCl-imi** and b) high-resolution N1s region.

Transmission electron microscopy (TEM) was used to investigate the morphology of **TSP-AlCl-imi** and **MWCNT-TSP-AlCl-imi** (**Figure 6**). TEM micrographs (**Figure 6a-c**) show that **TSP-AlCl-imi** forms a series of compact and large aggregates. In contrast, in the case of **MWCNT-TSP-AlCl-imi** (**Figure 6e, f**), MWCNTs offer a framework for the formation of individual nanoobject. Therefore, the comparison between the TEM images of the two different systems highlights how MWCNTs behaves as suitable support material since they result uniformly wrapped by the copolymeric coverage along their whole surface. This is of particular importance for the properties of **MWCNT-TSP-AlCl-imi**, especially in term of surface area and accessibility of the reagents to active sites.

The first evidences highlighted by the TEM images analysis were corroborated by the nitrogen adsorption/desorption measurements carried out on pristine MWCNTs, **TSP-AlCl-imi**, and **MWCNT-TSP-AlCl-imi**. Specific surface area (SSA), estimated using the Brunauer-Emmett-Teller (BET) equation,[88] showed that **TSP-AlCl-imi** possess a very low SSA (<1 m^2/g). On the contrary, the immobilization of the copolymeric matrix onto MWCNTs to obtain **MWCNT-TSP-AlCl-imi**, allowed to reach a higher SSA of 216 m^2/g (**Figure S7**), being 238 m^2/g the SSA of pristine MWCNTs (**Figure S8**).

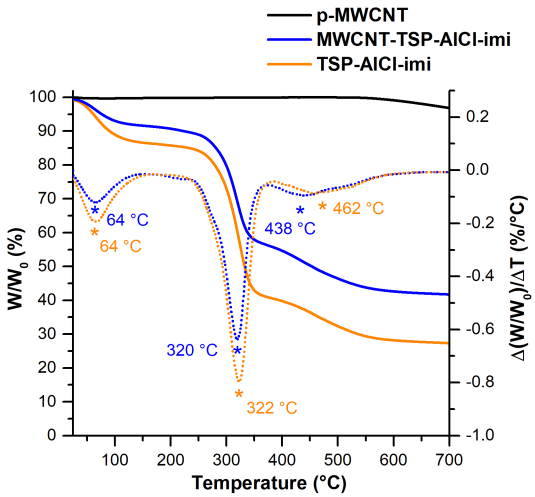

Fig. 5 TGA (solid lines) under N_2 flow and DTG (dotted lines) of pristine MWCNT (black line), **TSP-AlCl-imi** (orange lines) and **MWCNT-TSP-AlCl-imi** (blue lines).

Once characterized, both **TSP-AlCl-imi** and **MWCNT-TSP-AlCl-imi** materials were tested in the conversion of carbon dioxide into cyclic carbonates using styrene oxide as target epoxide under solvent free conditions and without the addition of any co-catalytic species. The comparison of their catalytic activities was studied using an equal mass amount of both materials as illustrated in **Scheme 2**. Conversions of 49% and 55% into the corresponding cyclic carbonate were obtained using **TSP-AlCl-imi** and **MWCNT-TSP-AlCl-imi**, respectively.

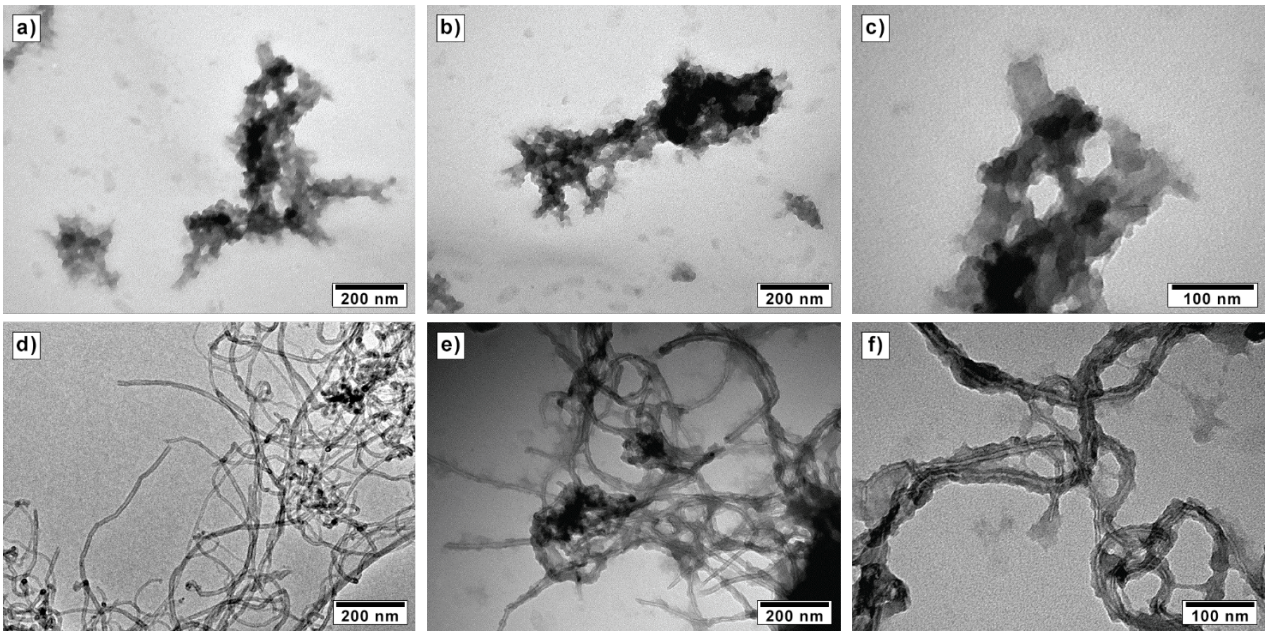

Fig. 6 TEM micrographs of a-c) **TSP-AlCl-imi**, d) pristine MWCNTs, and e, f) **MWCNT-TSP-AlCl-imi**.

However, due to the different content of active species in the two materials, a more accurate comparison of the performances of **TSP-AlCl-imi** and **MWCNT-TSP-AlCl-imi** catalytic systems was carried out taking into account the turnover number (TON; defined as moles of epoxide converted/moles of active sites) and turnover frequency (TOF; TON/reaction time in hours) values. The results, reported in **Scheme 2**, showed

that **MWCNT-TSP-AlCl-imi** possesses higher catalytic activity than **TSP-AlCl-imi** in the conversion of styrene oxide. TON_{Al} and TOF_{Al} values (7649, and 2550 h^{-1}) of **MWCNT-TSP-AlCl-imi** are about twice as high as those of **TSP-AlCl-imi** (3868 and 1289 h^{-1}). These findings further emphasize the importance of the use of MWCNTs as support material for the performance improvement of the catalytic material. The optimal morphology of **MWCNT-TSP-AlCl-imi,** which possess a high surface area and fully accessible catalytic sites, can be ascribed as the reason of its higher activity. Conversely, the unsupported copolymer **TSP-AlCl-imi** revealed to be a less active catalyst due to its low surface area that hinders the access of the reactants to the catalytic centers.

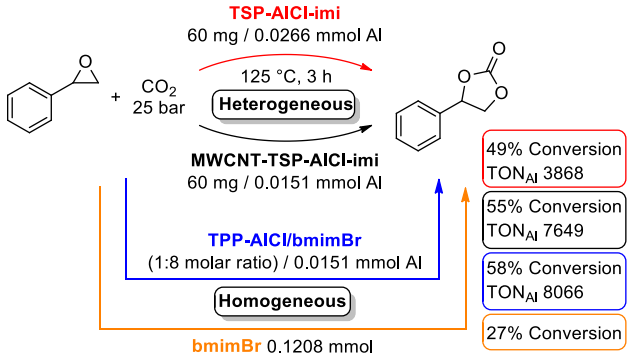

Scheme 2 Comparison of the activity between the heterogenous catalysts **TSP-AlCl-imi** and **MWCNT-TSP-AlCl-imi**, and the homogenous system **TPP-AlCl/bmimBr** and **bmimBr** in the reaction of styrene oxide with CO_2. Reaction conditions: styrene oxide (217 mmol), catalyst (0.0266 or 0.0151 mmol Al), 25 bar CO_2, 125 ºC, 3 h, 500 rpm.

Two additional experiments in which tetraphenylporphyrin aluminum chloride complex **TPP-AlCl** with the addition of 1-butyl-3-methylimidazolium bromide (bmimBr) as source of Br^- (Al/Br^- molar ratio 1:8) or only bmimBr were used as homogeneous catalytic systems were carried out (**Scheme 2**). The aluminum loading used for the reaction in homogenous conditions was the same employed in the case of **MWCNT-TSP-AlCl-imi**, namely 0.0151 mmol. Interestingly, **MWCNT-TSP-AlCl-imi** showed an activity comparable to that of **TPP-AlCl/bmimBr** homogeneous system with conversion values of 55% and 58%, respectively. On the contrary, the reaction catalyzed by the Lewis base species alone (bmimBr) reached a much lower conversion of 27%. For the sake of completeness, a blank test with just MWCNTs have been also carried out showing no conversion of the epoxide. The outstanding performance of **MWCNT-TSP-AlCl-imi** could be ascribed to the fine control achieved over the relative position of the two different catalytic sites (aluminium and bromide ions) which is missing in the case of the homogeneous **TPP-AlCl/bmimBr** mixture, that represent a more disordered system. The structure of the supported polymeric network formed by the linkage between the porphyrin core and the bis-vinylimidazolium salt ensures the close proximity between the metal centers and the bromide ions, which are able to cooperate and exert a synergistic effect during the catalytic cycle for the formation of the cyclic carbonate, as depicted in **Scheme 3**. In the step A, the oxygen atom of the epoxide interacts with the Lewis acidic aluminum site of the porphyrin core with the formation of a coordination complex, which is attacked by the nucleophile (Br^-) on the less-hindered side of epoxide to afford the Al-

coordinated bromo alkoxide (step B). Subsequently, the insertion of CO_2 into the Al–O bond gave rise to a metal coordinated carbonate (step C), which undergoes to an intramolecular SN_2 cyclization with the release of a bromide ion, which regenerate the catalyst, and the concomitant formation of the cyclic carbonate (step D). Therefore, **MWCNT-TSP-AlCl-imi** has proved to be a promising catalyst both from the point of view of its morphology, which ensure a high accessibility to the reactants, and of its molecular structure, which lead to an increase of the catalytic activity thank to the cooperation/synergism between the electrophilic and nucleophilic sites.

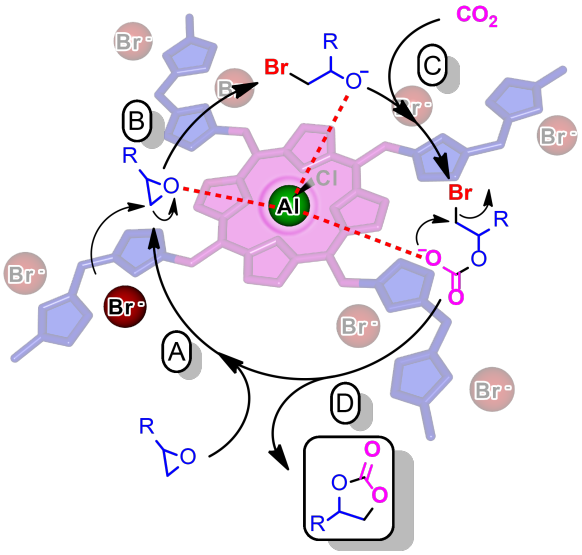

Scheme 3. Representation of the synergy between the Lewis acid and the bromide ion in the prepared bifunctional catalysts for the synthesis of cyclic carbonates.

The recyclability of both heterogeneous catalysts in the styrene oxide conversion was studied. Five consecutive runs were carried out and after each cycle the materials were easily recovered by centrifugation and washed with toluene, ethanol, and diethyl ether without any additional activation treatment. The results, showed in **Figure 7** and **Figure S9**, highlighted that both catalysts revealed to be robust and able to be used for multiple cycles without any decrease of their catalytic activity.

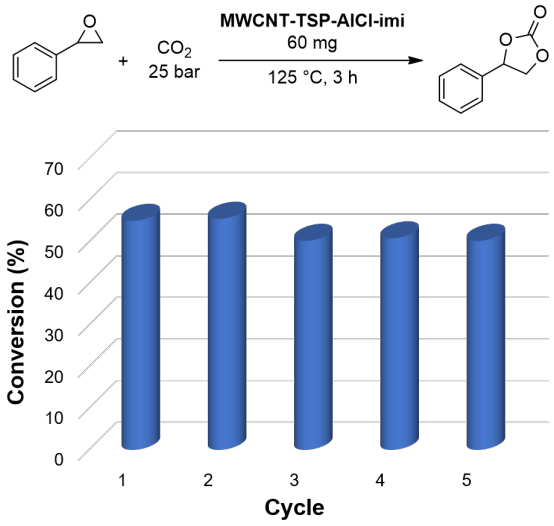

Fig.7 Recycling test of **MWCNT-TSP-AlCl-Imi**. Reaction conditions: styrene oxide (217 mmol), 60 mg **MWCNT-TSP-AlCl-Imi** (0.0151 mmol Al), 25 bar CO_2, 3 h, 500 rpm.

Interestingly, the high-resolution XPS spectrum of the N1s region of the used **MWCNT-TSP-AlCl-imi** after the recycling tests showed that the catalyst was not affected by any notable alteration since the atomic percentages of the two different nitrogen atoms remained almost unchanged with respect to the fresh **MWCNT-TSP-AlCl-imi** (**Figures 4b** and **S10**).

More in-depth studies to exclude the presence in solution of catalytically active species at the end of the reaction were undertaken. The more active **MWCNT-TSP-AlCl-imi** catalyst was subjected to a leaching test in the reaction of CO_2 with styrene oxide. At the end of the reaction, the material was removed by centrifugation and the liquid phase was again reacted in the same reaction conditions. The graph of the variation of CO_2 pressure during the reaction time (**Figure S11**) showed that an almost constant pressure of carbon dioxide was maintained during the reaction. This finding was also confirmed by ^{1}H NMR analysis of the reaction mixture that showed only a 1.5% increase in the conversion of the styrene oxide into styrene carbonate confirming the absence of leached species in solution.

Table 1 Cyclic carbonates synthesis catalyzed by **MWCNT-TSP-AlCl-imi**.

Entry	Substrate	t (h)	T (°C)	Conversion (%)[a]	TON_{Al}[b]	TOF_{Al} (h^{-1})[b]
1	 210 mmol	3	125	55	7,649	2,550
2[c]		20		84	23,426	1,171
3[c]		18	150	>95	26,773	1,487
4	 306 mmol	3	50	18	3,648	1,216
5			80	83	16,820	5,607
6			100	>95	20,265	6,755
7[d]	 306 or 379 mmol	3	30	31	6,282	2,094
8[d,e]			30	26	5,269	1,756
9[f]			50	62	15,562	5,187
10[f]		5	50	83	20,832	4,166
11[f]		10	50	91	22,840	2,284
12	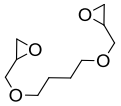 131 mmol	20	125	>95	16,483	824
13[g]	 237 mmol	24	150	71[h]	3,352	140

Reaction conditions: CO_2 (25 bar), catalyst 60 mg (0.0151 mmol Al), 500 rpm. [a] Determined by ^{1}H NMR (see **Figures S12-20**). [b] TON and TOF values calculated on the basis of the Al content obtained from ICP analysis. [c] Catalyst 30 mg (0.0075 mmol Al). [d] 306 mmol of glycidol were used. [e] CO_2 constant pressure 10

bar. [f] 379 mmol of glycidol were used. [g] Catalyst 200 mg (0.0502 mmol Al). [h] Selectivity toward cyclic carbonates 74% (*cis*/*trans* ratio 65:35) [i] Catalyst 240 mg (0.0602 mmol Al).

Once verified both the recyclability and the absence of any leaching, the substrate scope of **MWCNT-TSP-AlCl-imi** catalyst was further explored using, in addition to styrene oxide, a series of epoxides including epichlorohydrin, glycidol, and 1,4-butanediol diglycidyl ether (**Table 1**, **entries 1-12**). Some of the catalytic tests were repeated thus confirming the good reproducibility of the experiments and indicating that the error associated to the catalytic data can be estimated in the range of + 2%. As shown in **Scheme 2** styrene oxide was transformed into the corresponding cyclic carbonate with a conversion of 55% when **MWCNT-TSP-AlCl-imi** (0.0151 mmol Al) was employed at 125 °C and with a reaction time of 3 h (**Entry 1**). However, the reduction of the catalytic loading by half (0.0075 mmol Al) and the extension of the reaction time up to 20 h resulted in the increase of the conversion of styrene oxide up to 84 % with a TON value of 23,426 (**Entry 2**). In addition, full conversion (>95%) was reached in 18 h by increasing the reaction temperature up to 150 °C affording a TON value of 26,773 (**Entry 3**). The reactivity of epichlorohydrin was explored at three different temperatures, namely 50, 80, and 100 °C (**Entries 4-6**), applying a reaction time of 3 h and a catalytic loading of 0.0151 mmol Al. The conversion values ranged from 18% at 50 °C to >95% when the temperature was increased up to 100 °C. Moderate conversion values of the more reactive glycidol was obtained at 30 °C in 3 h, with only small differences when an initial CO_2 pressure of 25 bar or a constant pressure of 10 bar was applied (**Entries 7** and **8**). Conversely, the increase of the temperature up to 50 °C with the same reaction time gave rise to 62% conversion of glycidol (**Entry 9**). A longer reaction time (5 h) allowed to obtain a higher conversion of 83% into the corresponding cyclic carbonate (**Entry 10**). However, a longer reaction time (10 h) produced only a little increase of the conversion up to 91% (**Entry 11**), indicating that the kinetic of this reaction strongly decreased with the increasing conversion. 1,4-butanediol diglycidyl ether was successfully converted into the corresponding cyclic carbonate at 125 °C after 20 h (**Entry 12**). The outstanding results obtained encouraged us to test **MWCNT-TSP-AlCl-imi** with the less reactive cyclohexene oxide. Cyclohexene oxide displayed a 71% conversion when the reaction was carried out at 150 °C for 24 h (**Entry 13**). However, the *cis*-cyclohexene carbonate was not the only product obtained and poly(cyclohexene carbonate) and *trans*-cyclohexene carbonate, the latter formed by back-biting reaction that can occur at the end of the growing polymer chain,[89, 90] were also detected. ^{1}H NMR spectrum of the reaction mixture (**Figure S20**) allowed to calculate the selectivity toward the cyclic carbonates products by integrating the signals attributed to the methylene groups of the different products. Under the selected reaction conditions, a quasi linear dependence from the pressure of CO_2 was observed. An example of this behavior in the presence of epichlorohydrin is reported in **Figure S21**.

Finally, the remarkable catalytic activity of **MWCNT-TSP-AlCl-imi** is among the highest achieved by heterogeneous bifunctional (Lewis acid/X^-) catalysts in the cyclic carbonate synthesis.[47-69] In particular, **Table 2** compares the activity of previously reported heterogeneous bifunctional porphyrin-based catalytic systems with **MWCNT-TSP-AlCl-imi**, which proved to be highly competitive with other systems.

Table 2 Selected data for the reaction between epichlorohydrin and CO_2 in the presence of porphyrin-M-based heterogeneous bi-functional catalytic systems.

Entry	Catalyst	Yield (%)	TOF (h^{-1})	P[a]	P/h (h^{-1})	Conditions	Ref.
1	**MWCNT-TSP-AlCl-imi**	>99	6755	696	232	3 h, 100 °C, 2.5 MPa	This work
2	**Al-iPOP-2**	>99	167	89	15	6 h, 40 °C, 1.0 MPa	[55]
3	**BIO-1c**	91	910	11	11	1 h, 120 °C, 1.7 MPa	[63]
4	**ZnTPy-BIM4/CNTs-3**	98	528 (1842)[b]	10	4	2.5 h, 120 °C, 1.5 MPa	[54]
5	**SYSU-Zn@IL2**	>99	52	34	3	12 h, 80 °C, 1.0 MPa	[53]
6	**Zn-ClF2-C_2H_4**	98	136	30	7	4 h, 120 °C, 2.5 MPa	[50]
7	**Mg-por/pho@POP**	67	13400	293	293	1 h, 140 °C, 3.0 MPa	[49]
8	**ZnTPP/QA-azo-PiP_1**	>99	33	29	2	12 h, 80 °C, 1.0 MPa	[64]
9	**ZnPor-CP**	93	73	38	2	16 h, 100 °C, 1.0 MPa	[65]
10	**CoTPP-PiP(Br)**	>99	42	64	5	12 h, 80 °C, 1.0 MPa	[66]
11	**[Zn(II)NMeTPyP]$^{4+}$ [I^-]$_4$@PCN-224**	>99	35	27	1	24 h, 90 °C, 0.8 MPa	[67]
12	**PP-Br-Zn-0.09**	94	528 (4080)[c]	23	12	2 h, 100 °C, 1.5 MPa	[68]
13	**SBA-Zn-TPy$^+$PBr$^-$$_{DMF}$**	>99	286 (685)[d]	25	7	3.5 h, 120 °C, 1.5 MPa	[69]

[a] Productivity: calculated as $g_{carbonate}/g_{catalyst}$. [b] TOF was calculated with the conversion below 35% and S/C = 7100. [c] TOF was calculated with the conversion below 35%. [d] TOF was calculated with the conversion below 35% and S/C = 2000.

Conclusions

Aluminum chloride tetrastyrylporphyrin (**TSP-Al-Cl**) and 1,4-butanediyl-3,3′-bis-1-vinylimidazolium dibromide have been subjected to AIBN-mediated radical polymerization in the presence (**MWCNT-TSP-AlCl-imi**) and in absence (**TSP-AlCl-imi**) of multi-walled carbon nanotubes (MWCNTs). The corresponding crosslinked materials have been thoroughly characterized by means of several spectroscopic and analytic techniques such as TGA, ICP-OES, FT-IR, XPS, TEM, solid state NMR, porosimetry. The hybrid materials have been employed as heterogeneous catalysts in the cycloaddition reaction of CO_2 to epoxides to afford the corresponding cyclic carbonates under solvent-free conditions, resulting **MWCNT-TSP-AlCl-imi** the most active with TON and TOF double than those obtained with the unsupported one. The enhanced activity of the nanocarbon-based catalyst can be ascribed to its higher surface area that permits fully accessible catalytic sites, in comparison with the very low SSA of **TSP-AlCl-imi** (<1 m^2/g). Moreover, the heterogeneous **MWCNT-TSP-AlCl-imi** system displays a catalytic activity very similar to that of a reference homogeneous catalytic mixture comprised of aluminium tetraphenylporphyrin and bmimBr. This outstanding performance could be ascribed to the fine control achieved over the relative position of the catalytic sites given that the direct covalent linking between the porphyrin core and the bis-vinylimidazolium salt ensures the close proximity between the metal centers and the bromide ions, which are able to cooperate

and exert a synergistic effect during the catalytic cycle. The hybrid catalyst showed an excellent catalytic activity, among the highest ever reported for a bifunctional material, with a set of different epoxides, with TON and TOF values of up to 28,900 and 8,366, respectively. **MWCNT-TSP-AlCl-imi** was easily recoverable and recyclable for at least five cycles with unchanged activity, and no leaching phenomena have been observed during the performed tests. This promising material pave the way toward the setting up of a family of robust and recyclable catalysts to be used both in batch and in flow systems. Most performing materials could be prepared by changing both the kind of metalloporphyrin as well as the anion of the poly-ionic liquid network. Such work will be reported in due course.

CRediT authorship contribution statement

Vincenzo Campisciano: Investigation, Writing- Original draft preparation, Visualization. **Laura Valentino:** Investigation, Data curation. **Anthony Morena:** Investigation, Data curation. **Andrea Santiago Portillo:** Investigation, Data curation, Writing- Original draft preparation. **Nicolò Saladino**: Investigation, Data curation. **Michelangelo Gruttadauria***:* Conceptualization, Supervision**. Carmela Aprile**: Methodology, Validation, Funding Acquisition. **Francesco Giacalone:** Conceptualization, Methodology, Validation, Funding Acquisition.

Conflicts of interest

There are no conflicts to declare.

Acknowledgements

The authors gratefully acknowledge the University of Palermo and the Italian Ministry of Education, University and Research (MIUR) for financial support through PRIN 2017 (project no. 2017W8KNZW). Also, the authors acknowledge the University of Namur for postdoctoral fellowship. This research is supported by the F.R.S-FNRS via the funding grants GEQ U.G014.19 and EQP U.N034.17. This research used resources of the PC2 and the MORPH-IM platforms located at the University of Namur. A. M. gratefully acknowledges the University of Palermo and University of Namur for a co-funded PhD fellowship.

References

[1] A. Dibenedetto, A. Angelini, P. Stufano, Use of carbon dioxide as feedstock for chemicals and fuels: homogeneous and heterogeneous catalysis, J. Chem. Technol. Biotechnol., 89 (2014) 334-353.

[2] K.M.K. Yu, I. Curcic, J. Gabriel, S.C.E. Tsang, Recent Advances in CO2 Capture and Utilization, ChemSusChem, 1 (2008) 893-899.

[3] J. Artz, T.E. Müller, K. Thenert, J. Kleinekorte, R. Meys, A. Sternberg, A. Bardow, W. Leitner, Sustainable Conversion of Carbon Dioxide: An Integrated Review of Catalysis and Life Cycle Assessment, Chem. Rev., 118 (2018) 434-504.

[4] M. Aresta, A. Dibenedetto, A. Angelini, Catalysis for the Valorization of Exhaust Carbon: from CO2 to Chemicals, Materials, and Fuels. Technological Use of CO2, Chem. Rev., 114 (2014) 1709-1742.
[5] W. Clegg, R.W. Harrington, M. North, F. Pizzato, P. Villuendas, Cyclic carbonates as sustainable solvents for proline-catalysed aldol reactions, Tetrahedron: Asymmetry, 21 (2010) 1262-1271.
[6] J.H. Clements, Reactive Applications of Cyclic Alkylene Carbonates, Ind. Eng. Chem. Res., 42 (2003) 663-674.
[7] B. Schäffner, F. Schäffner, S.P. Verevkin, A. Börner, Organic Carbonates as Solvents in Synthesis and Catalysis, Chem. Rev., 110 (2010) 4554-4581.
[8] V.B. Saptal, B.M. Bhanage, Current advances in heterogeneous catalysts for the synthesis of cyclic carbonates from carbon dioxide, Curr. Opin. Green Sustain. Chem., 3 (2017) 1-10.
[9] F. Della Monica, A. Buonerba, C. Capacchione, Homogeneous Iron Catalysts in the Reaction of Epoxides with Carbon Dioxide, Adv. Synth. Catal., 361 (2019) 265-282.
[10] R. Luo, X. Liu, M. Chen, B. Liu, Y. Fang, Recent Advances on Imidazolium-Functionalized Organic Cationic Polymers for CO2 Adsorption and Simultaneous Conversion into Cyclic Carbonates, ChemSusChem, 13 (2020) 3945-3966.
[11] R. Luo, M. Chen, X. Liu, W. Xu, J. Li, B. Liu, Y. Fang, Recent advances in CO2 capture and simultaneous conversion into cyclic carbonates over porous organic polymers having accessible metal sites, J. Mater. Chem. A, 8 (2020) 18408-18424.
[12] L. Guo, K.J. Lamb, M. North, Recent developments in organocatalysed transformations of epoxides and carbon dioxide into cyclic carbonates, Green Chem., 23 (2021) 77-118.
[13] K. Tomishige, Y. Gu, Y. Nakagawa, M. Tamura, Reaction of CO2 With Alcohols to Linear-, Cyclic-, and Poly-Carbonates Using CeO2-Based Catalysts, Front. Energy Res., 8 (2020) 117.
[14] K.B. Rasal, G.D. Yadav, R. Koskinen, R. Keiski, Solventless synthesis of cyclic carbonates by direct utilization of CO2 using nanocrystalline lithium promoted magnesia, Mol. Catal., 451 (2018) 200-208.
[15] A.H. Chowdhury, P. Bhanja, N. Salam, A. Bhaumik, S.M. Islam, Magnesium oxide as an efficient catalyst for CO2 fixation and N-formylation reactions under ambient conditions, Mol. Catal., 450 (2018) 46-54.
[16] N. Kulal, V. Vasista, G.V. Shanbhag, Identification and tuning of active sites in selected mixed metal oxide catalysts for cyclic carbonate synthesis from epoxides and CO2, J. CO2 Util., 33 (2019) 434-444.
[17] D. Prasad, K.N. Patil, R.B. Dateer, H. Kim, B.M. Nagaraja, A.H. Jadhav, Basicity controlled MgCo2O4 nanostructures as catalyst for viable fixation of CO2 into epoxides at atmospheric pressure, Chem. Eng. J., 405 (2021) 126907.
[18] P.-Z. Li, X.-J. Wang, J. Liu, J.S. Lim, R. Zou, Y. Zhao, A Triazole-Containing Metal–Organic Framework as a Highly Effective and Substrate Size-Dependent Catalyst for CO2 Conversion, J. Am. Chem. Soc., 138 (2016) 2142-2145.
[19] J. Liang, Y.-B. Huang, R. Cao, Metal–organic frameworks and porous organic polymers for sustainable fixation of carbon dioxide into cyclic carbonates, Coord. Chem. Rev., 378 (2019) 32-65.
[20] S. Huh, Direct Catalytic Conversion of CO2 to Cyclic Organic Carbonates under Mild Reaction Conditions by Metal—Organic Frameworks, Catalysts, 9 (2019) 34.
[21] T.K. Pal, D. De, P.K. Bharadwaj, Metal–organic frameworks for the chemical fixation of CO2 into cyclic carbonates, Coord. Chem. Rev., 408 (2020) 213173.
[22] S. Singh Dhankhar, B. Ugale, C.M. Nagaraja, Co-Catalyst-Free Chemical Fixation of CO2 into Cyclic Carbonates by using Metal-Organic Frameworks as Efficient Heterogeneous Catalysts, Chem. - Asian J., 15 (2020) 2403-2427.
[23] P.T.K. Nguyen, H.T.D. Nguyen, H.N. Nguyen, C.A. Trickett, Q.T. Ton, E. Gutiérrez-Puebla, M.A. Monge, K.E. Cordova, F. Gándara, New Metal–Organic Frameworks for Chemical Fixation of CO2, ACS Appl. Mater. Interfaces, 10 (2018) 733-744.
[24] C.-G. Li, L. Xu, P. Wu, H. Wu, M. He, Efficient cycloaddition of epoxides and carbon dioxide over novel organic–inorganic hybrid zeolite catalysts, Chem. Commun., 50 (2014) 15764-15767.
[25] B. Mousavi, S. Chaemchuen, B. Moosavi, Z. Luo, N. Gholampour, F. Verpoort, Zeolitic imidazole framework-67 as an efficient heterogeneous catalyst for the conversion of CO2 to cyclic carbonates, New J. Chem., 40 (2016) 5170-5176.

[26] B. Sarmah, B. Satpati, R. Srivastava, Highly efficient and recyclable basic mesoporous zeolite catalyzed condensation, hydroxylation, and cycloaddition reactions, J. Colloid Interface Sci., 493 (2017) 307-316.
[27] Q.-N. Zhao, Q.-W. Song, P. Liu, Q.-X. Zhang, J.-H. Gao, K. Zhang, Catalytic Conversion of CO2 to Cyclic Carbonates through Multifunctional Zinc-Modified ZSM-5 Zeolite, Chin. J. Chem . 36 (2018) 187-193.
[28] R. Babu, S.-H. Kim, J.F. Kurisingal, H.-J. Kim, G.-G. Choi, D.-W. Park, A room temperature synthesizable zeolitic imidazolium framework catalyst for the solvent-free synthesis of cyclic carbonates, J. CO2 Util., 25 (2018) 6-13.
[29] K.M. Bhin, J. Tharun, K.R. Roshan, D.-W. Kim, Y. Chung, D.-W. Park, Catalytic performance of zeolitic imidazolate framework ZIF-95 for the solventless synthesis of cyclic carbonates from CO2 and epoxides, J. CO2 Util., 17 (2017) 112-118.
[30] R. Duan, C. Hu, Y. Zhou, Y. Huang, Z. Sun, H. Zhang, X. Pang, Propylene Oxide Cycloaddition with Carbon Dioxide and Homopolymerization: Application of Commercial Beta Zeolites, Ind. Eng. Chem. Res., 60 (2021) 1210-1218.
[31] K. Huang, J.-Y. Zhang, F. Liu, S. Dai, Synthesis of Porous Polymeric Catalysts for the Conversion of Carbon Dioxide, ACS Catal., 8 (2018) 9079-9102.
[32] J. Ozdemir, I. Mosleh, M. Abolhassani, L.F. Greenlee, R.R. Beitle, M.H. Beyzavi, Covalent Organic Frameworks for the Capture, Fixation, or Reduction of CO2, Front. Energy Res., 7 (2019) 77.
[33] V. Campisciano, C. Calabrese, F. Giacalone, C. Aprile, P. Lo Meo, M. Gruttadauria, Reconsidering TOF calculation in the transformation of epoxides and CO2 into cyclic carbonates, J. CO2 Util., 38 (2020) 132-140.
[34] W. Wang, C. Li, J. Jin, L. Yan, Y. Ding, Mg–porphyrin complex doped divinylbenzene based porous organic polymers (POPs) as highly efficient heterogeneous catalysts for the conversion of CO2 to cyclic carbonates, Dalton Trans., 47 (2018) 13135-13141.
[35] D. Chen, R. Luo, M. Li, M. Wen, Y. Li, C. Chen, N. Zhang, Salen(Co(iii)) imprisoned within pores of a metal–organic framework by post-synthetic modification and its asymmetric catalysis for CO2 fixation at room temperature, Chem. Commun., 53 (2017) 10930-10933.
[36] Y. Fan, J. Li, Y. Ren, H. Jiang, A Ni(salen)-Based Metal–Organic Framework: Synthesis, Structure, and Catalytic Performance for CO2 Cycloaddition with Epoxides, Eur. J. Inorg. Chem., 2017 (2017) 4982-4989.
[37] C.K. Ng, R.W. Toh, T.T. Lin, H.-K. Luo, T.S.A. Hor, J. Wu, Metal–salen molecular cages as efficient and recyclable heterogeneous catalysts for cycloaddition of CO2 with epoxides under ambient conditions, Chem. Sci., 10 (2019) 1549-1554.
[38] L. Hu, Q. Xie, J. Tang, C. Pan, G. Yu, K.C. Tam, Co(III)-Salen immobilized cellulose nanocrystals for efficient catalytic CO2 fixation into cyclic carbonates under mild conditions, Carbohydr. Polym., 256 (2021) 117558.
[39] Z. Dai, Q. Sun, X. Liu, C. Bian, Q. Wu, S. Pan, L. Wang, X. Meng, F. Deng, F.-S. Xiao, Metalated porous porphyrin polymers as efficient heterogeneous catalysts for cycloaddition of epoxides with CO2 under ambient conditions, J. Catal., 338 (2016) 202-209.
[40] S. Wang, K. Song, C. Zhang, Y. Shu, T. Li, B. Tan, A novel metalporphyrin-based microporous organic polymer with high CO2 uptake and efficient chemical conversion of CO2 under ambient conditions, J. Mater. Chem. A, 5 (2017) 1509-1515.
[41] Y. Qin, H. Guo, X. Sheng, X. Wang, F. Wang, An aluminum porphyrin complex with high activity and selectivity for cyclic carbonate synthesis, Green Chem., 17 (2015) 2853-2858.
[42] A. Chen, Y. Zhang, J. Chen, L. Chen, Y. Yu, Metalloporphyrin-based organic polymers for carbon dioxide fixation to cyclic carbonate, J. Mater. Chem. A, 3 (2015) 9807-9816.
[43] M.H. Kim, T. Song, U.R. Seo, J.E. Park, K. Cho, S.M. Lee, H.J. Kim, Y.-J. Ko, Y.K. Chung, S.U. Son, Hollow and microporous catalysts bearing Cr(iii)–F porphyrins for room temperature CO2 fixation to cyclic carbonates, J. Mater. Chem. A, 5 (2017) 23612-23619.
[44] Y. Chen, R. Luo, Q. Xu, W. Zhang, X. Zhou, H. Ji, State-of-the-Art Aluminum Porphyrin-based Heterogeneous Catalysts for the Chemical Fixation of CO2 into Cyclic Carbonates at Ambient Conditions, ChemCatChem, 9 (2017) 767-773.

[45] J. Rintjema, A.W. Kleij, Aluminum-Mediated Formation of Cyclic Carbonates: Benchmarking Catalytic Performance Metrics, ChemSusChem, 10 (2017) 1274-1282.
[46] G.N. Bondarenko, E.G. Dvurechenskaya, O.G. Ganina, F. Alonso, I.P. Beletskaya, Solvent-free synthesis of cyclic carbonates from CO2 and epoxides catalyzed by reusable alumina-supported zinc dichloride, Appl. Catal. B: Environ., 254 (2019) 380-390.
[47] Z. Dai, Y. Tang, F. Zhang, Y. Xiong, S. Wang, Q. Sun, L. Wang, X. Meng, L. Zhao, F.-S. Xiao, Combination of binary active sites into heterogeneous porous polymer catalysts for efficient transformation of CO2 under mild conditions, Chin. J. Catal., 42 (2021) 618-626.
[48] J. Li, Y. Han, H. Lin, N. Wu, Q. Li, J. Jiang, J. Zhu, Cobalt–Salen-Based Porous Ionic Polymer: The Role of Valence on Cooperative Conversion of CO2 to Cyclic Carbonate, ACS Appl. Mater. Interfaces, 12 (2020) 609-618.
[49] W. Wang, Y. Wang, C. Li, L. Yan, M. Jiang, Y. Ding, State-of-the-Art Multifunctional Heterogeneous POP Catalyst for Cooperative Transformation of CO2 to Cyclic Carbonates, ACS Sustainable Chem. Eng., 5 (2017) 4523-4528.
[50] J. Liu, G. Zhao, O. Cheung, L. Jia, Z. Sun, S. Zhang, Highly Porous Metalloporphyrin Covalent Ionic Frameworks with Well-Defined Cooperative Functional Groups as Excellent Catalysts for CO2 Cycloaddition, Chem. - Eur. J., 25 (2019) 9052-9059.
[51] R. Luo, Y. Chen, Q. He, X. Lin, Q. Xu, X. He, W. Zhang, X. Zhou, H. Ji, Metallosalen-Based Ionic Porous Polymers as Bifunctional Catalysts for the Conversion of CO2 into Valuable Chemicals, ChemSusChem, 10 (2017) 1526-1533.
[52] T.-T. Liu, J. Liang, Y.-B. Huang, R. Cao, A bifunctional cationic porous organic polymer based on a Salen-(Al) metalloligand for the cycloaddition of carbon dioxide to produce cyclic carbonates, Chem. Commun., 52 (2016) 13288-13291.
[53] Y. Chen, R. Luo, Q. Xu, J. Jiang, X. Zhou, H. Ji, Metalloporphyrin Polymers with Intercalated Ionic Liquids for Synergistic CO2 Fixation via Cyclic Carbonate Production, ACS Sustainable Chem. Eng., 6 (2018) 1074-1082.
[54] S. Jayakumar, H. Li, J. Chen, Q. Yang, Cationic Zn–Porphyrin Polymer Coated onto CNTs as a Cooperative Catalyst for the Synthesis of Cyclic Carbonates, ACS Appl. Mater. Interfaces, 10 (2018) 2546-2555.
[55] Y. Chen, R. Luo, Q. Xu, J. Jiang, X. Zhou, H. Ji, Charged Metalloporphyrin Polymers for Cooperative Synthesis of Cyclic Carbonates from CO2 under Ambient Conditions, ChemSusChem, 10 (2017) 2534-2541.
[56] P. Puthiaraj, S. Ravi, K. Yu, W.-S. Ahn, CO2 adsorption and conversion into cyclic carbonates over a porous ZnBr2-grafted N-heterocyclic carbene-based aromatic polymer, Appl. Catal. B: Environ., 251 (2019) 195-205.
[57] K. Naveen, H. Ji, T.S. Kim, D. Kim, D.-H. Cho, C3-symmetric zinc complexes as sustainable catalysts for transforming carbon dioxide into mono- and multi-cyclic carbonates, Appl. Catal. B: Environ., 280 (2021) 119395.
[58] S.A. Kuznetsova, Y.A. Rulev, V.A. Larionov, A.F. Smol'yakov, Y.V. Zubavichus, V.I. Maleev, H. Li, M. North, A.S. Saghyan, Y.N. Belokon, Self-Assembled Ionic Composites of Negatively Charged Zn(salen) Complexes and Triphenylmethane Derived Polycations as Recyclable Catalysts for the Addition of Carbon Dioxide to Epoxides, ChemCatChem, 11 (2019) 511-519.
[59] P.A. Carvalho, J.W. Comerford, K.J. Lamb, M. North, P.S. Reiss, Influence of Mesoporous Silica Properties on Cyclic Carbonate Synthesis Catalysed by Supported Aluminium(Salen) Complexes, Adv. Synth. Catal., 361 (2019) 345-354.
[60] Q. Yi, T. Liu, X. Wang, Y. Shan, X. Li, M. Ding, L. Shi, H. Zeng, Y. Wu, One-step multiple-site integration strategy for CO2 capture and conversion into cyclic carbonates under atmospheric and cocatalyst/metal/solvent-free conditions, Appl. Catal. B: Environ., 283 (2021) 119620.
[61] R. Luo, W. Zhang, Z. Yang, X. Zhou, H. Ji, Synthesis of cyclic carbonates from epoxides over bifunctional salen aluminum oligomers as a CO2-philic catalyst: Catalytic and kinetic investigation, J. CO2 Util., 19 (2017) 257-265.

[62] C. Martín, C.J. Whiteoak, E. Martin, M. Martínez Belmonte, E.C. Escudero-Adán, A.W. Kleij, Easily accessible bifunctional Zn(salpyr) catalysts for the formation of organic carbonates, Catal. Sci. Technol., 4 (2014) 1615-1621.
[63] T. Ema, Y. Miyazaki, T. Taniguchi, J. Takada, Robust porphyrin catalysts immobilized on biogenous iron oxide for the repetitive conversions of epoxides and CO2 into cyclic carbonates, Green Chem., 15 (2013) 2485-2492.
[64] Y. Chen, Q. Ren, X. Zeng, L. Tao, X. Zhou, H. Ji, Sustainable synthesis of multifunctional porous metalloporphyrin polymers for efficient carbon dioxide transformation under mild conditions, Chem. Eng. Sci., 232 (2021) 116380.
[65] X. Liu, F. Zhou, M. Chen, W. Xu, H. Liu, J. Zhong, R. Luo, Synergistically Converting Carbon Dioxide into Cyclic Carbonates by Metalloporphyrin-Based Cationic Polymers with Imidazolium Functionality, ChemistrySelect, 6 (2021) 583-588.
[66] Y. Chen, R. Luo, Q. Ren, X. Zhou, H. Ji, Click-Based Porous Ionic Polymers with Intercalated High-Density Metalloporphyrin for Sustainable CO2 Transformation, Ind. Eng. Chem. Res., 59 (2020) 20269-20277.
[67] N. Sharma, S.S. Dhankhar, C.M. Nagaraja, Environment-friendly, co-catalyst- and solvent-free fixation of CO2 using an ionic zinc(ii)–porphyrin complex immobilized in porous metal–organic frameworks, Sustain. Energy Fuels, 3 (2019) 2977-2982.
[68] L. Liu, S. Jayakumar, J. Chen, L. Tao, H. Li, Q. Yang, C. Li, Synthesis of Bifunctional Porphyrin Polymers for Catalytic Conversion of Dilute CO2 to Cyclic Carbonates, ACS Appl. Mater. Interfaces, 13 (2021) 29522-29531.
[69] S. Jayakumar, H. Li, L. Tao, C. Li, L. Liu, J. Chen, Q. Yang, Cationic Zn-Porphyrin Immobilized in Mesoporous Silicas as Bifunctional Catalyst for CO2 Cycloaddition Reaction under Cocatalyst Free Conditions, ACS Sustainable Chem. Eng., 6 (2018) 9237-9245.
[70] C. Calabrese, L. Fusaro, L.F. Liotta, F. Giacalone, A. Comès, V. Campisciano, C. Aprile, M. Gruttadauria, Efficient Conversion of Carbon Dioxide by Imidazolium-Based Cross-Linked Nanostructures Containing Polyhedral Oligomeric Silsesquioxane (POSS) Building Blocks, ChemPlusChem, 84 (2019) 1536-1543.
[71] C. Calabrese, L.F. Liotta, F. Giacalone, M. Gruttadauria, C. Aprile, Supported Polyhedral Oligomeric Silsesquioxane-Based (POSS) Materials as Highly Active Organocatalysts for the Conversion of CO2, ChemCatChem, 11 (2019) 560-567.
[72] C. Calabrese, L.F. Liotta, E. Carbonell, F. Giacalone, M. Gruttadauria, C. Aprile, Imidazolium-Functionalized Carbon Nanohorns for the Conversion of Carbon Dioxide: Unprecedented Increase of Catalytic Activity after Recycling, ChemSusChem, 10 (2017) 1202-1209.
[73] M. Buaki-Sogó, A. Vivian, L.A. Bivona, H. García, M. Gruttadauria, C. Aprile, Imidazolium functionalized carbon nanotubes for the synthesis of cyclic carbonates: reducing the gap between homogeneous and heterogeneous catalysis, Catal. Sci. Technol., 6 (2016) 8418-8427.
[74] L.A. Bivona, O. Fichera, L. Fusaro, F. Giacalone, M. Buaki-Sogo, M. Gruttadauria, C. Aprile, A polyhedral oligomeric silsesquioxane-based catalyst for the efficient synthesis of cyclic carbonates, Catal. Sci. Technol., 5 (2015) 5000-5007.
[75] P. Agrigento, S.M. Al-Amsyar, B. Sorée, M. Taherimehr, M. Gruttadauria, C. Aprile, P.P. Pescarmona, Synthesis and high-throughput testing of multilayered supported ionic liquid catalysts for the conversion of CO2 and epoxides into cyclic carbonates, Catal. Sci. Technol., 4 (2014) 1598-1607.
[76] P. Agrigento, M.J. Beier, J.T.N. Knijnenburg, A. Baiker, M. Gruttadauria, Highly cross-linked imidazolium salt entrapped magnetic particles – preparation and applications, J. Mater. Chem., 22 (2012) 20728-20735.
[77] C. Aprile, F. Giacalone, P. Agrigento, L.F. Liotta, J.A. Martens, P.P. Pescarmona, M. Gruttadauria, Multilayered Supported Ionic Liquids as Catalysts for Chemical Fixation of Carbon Dioxide: A High-Throughput Study in Supercritical Conditions, ChemSusChem, 4 (2011) 1830-1837.
[78] V. Campisciano, R. Burger, C. Calabrese, L.F. Liotta, P. Lo Meo, M. Gruttadauria, F. Giacalone, Straightforward preparation of highly loaded MWCNT–polyamine hybrids and their application in catalysis, Nanoscale Adv., 2 (2020) 4199-4211.

[79] V. Campisciano, C. Calabrese, L.F. Liotta, V. La Parola, A. Spinella, C. Aprile, M. Gruttadauria, F. Giacalone, Templating effect of carbon nanoforms on highly cross-linked imidazolium network: Catalytic activity of the resulting hybrids with Pd nanoparticles, Appl. Organomet. Chem., 33 (2019) e4848.
[80] V. Campisciano, M. Gruttadauria, F. Giacalone, Modified Nanocarbons for Catalysis, ChemCatChem, 11 (2019) 90-133.
[81] J. Jiang, S. Yoon, A Metalated Porous Porphyrin Polymer with [Co(CO)4]− Anion as an Efficient Heterogeneous Catalyst for Ring Expanding Carbonylation, Sci. Rep., 8 (2018) 13243.
[82] X.Y. Li, M.Z. Zgierski, Porphine force field: in-plane normal modes of free-base porphine; comparison with metalloporphines and structural implications, J. Phys. Chem., 95 (1991) 4268-4287.
[83] Y.-H. Zhang, W.-J. Ruan, Z.-Y. Li, Y. Wu, J.-Y. Zheng, DFT study on the influence of meso-phenyl substitution on the geometric, electronic structure and vibrational spectra of free base porphyrin, Chem. Phys., 315 (2005) 201-213.
[84] J.O. Alben, S.S. Choi, A.D. Adler, W.S. Caughey, INFRARED SPECTROSCOPY OF PORPHYRINS*, Ann. N.Y. Acad. Sci., 206 (1973) 278-295.
[85] J.T. Mitchell-Koch, K.M. Padden, A.S. Borovik, Modification of immobilized metal complexes toward the design and synthesis of functional materials for nitric oxide delivery, J. Polym. Sci., Part A: Polym. Chem., 44 (2006) 2282-2292.
[86] S. Tait, R.A. Osteryoung, Infrared study of ambient-temperature chloroaluminates as a function of melt acidity, Inorg. Chem., 23 (1984) 4352-4360.
[87] K.R.J. Lovelock, I.J. Villar-Garcia, F. Maier, H.-P. Steinrück, P. Licence, Photoelectron Spectroscopy of Ionic Liquid-Based Interfaces, Chem. Rev., 110 (2010) 5158-5190.
[88] S. Brunauer, P.H. Emmett, E. Teller, Adsorption of Gases in Multimolecular Layers, J. Am. Chem. Soc., 60 (1938) 309-319.
[89] M. Cozzolino, F. Melchionno, F. Santulli, M. Mazzeo, M. Lamberti, Aldimine-Thioether-Phenolate Based Mono- and Bimetallic Zinc Complexes as Catalysts for the Reaction of CO2 with Cyclohexene Oxide, Eur. J. Inorg. Chem., (2020) 1645-1653.
[90] P.P. Pescarmona, M. Taherimehr, Challenges in the catalytic synthesis of cyclic and polymeric carbonates from epoxides and CO2, Catal. Sci. Technol., 2 (2012) 2169-2187.